© 2003 The Chemical Society of Japan

Alkylthio-functionalized Polymers Containing Alternating Phenylene and Thiophenediyl/Bithiophenediyl Repeating Units: the Synthesis and Characterization

Jingmei Xu, Siu Choon Ng, and Hardy Sze On Chan*

Department of Chemistry, National University of Singapore, Singapore 119260

(Received July 8, 2002)

Alkylthio(SR)-functionalized polymers poly(3-alkylthio-2,5-thiophenediyl-1,4-phenylene-*alt*-4-alkylthio-2,5-thiophenediyl-1,4-phenylene) (**P1**, alkyl = butyl, octyl and dodecyl) and poly[4,4′-bis(alkylthio)-2,2′-bithiophene-5,5′-diyl-*alt*-1,4-phenylene] (**P2**, alkyl = butyl, octyl and dodecyl) have been synthesized by Grignard coupling and $FeCl_3$ oxidation methods, respectively. Spectral measurements indicate that they are highly fluorescent, with quantum yields comparable to those of their alkyl(R)-functionalized analogues, poly(3-alkyl-2,5-thiophenediyl-1,4-phenylene-*alt*-4-alkyl-2,5-thiophenediyl-1,4-phenylene) (**P1′**, alkyl = butyl, octyl and dodecyl) and poly(4,4′-dialkyl-2,2′-bithiophene-5,5′-diyl-*alt*-1,4-phenylene) (**P2′**, alkyl = butyl, octyl and dodecyl). **P1** and **P2** are thermally less stable than **P1′** and **P2′**, because of the alkylthio group instead of an alkyl group. Modulated differential scanning calorimetry (MDSC) studies reveal a plasticizing effect exerted by the long side chains on the glass transitions (T_g) of the polymers. The **P2** series of polymers exhibit a much higher T_g than the **P1** series, ascribable to a greater resistance to segmental rotation in the former structure. A cyclic voltammetric study of polymers indicates that they are *n*-dopable. When doped by I_2 or $FeCl_3$, high doping levels of the polymers can be deduced from the weight change, XPS and elemental analysis, but conductivities are not high.

Conjugated polymers exhibit interesting electrical, electrochemical and optical properties because of their spatially extended π system. However, unsubstituted conjugated polymers are insoluble and infusible. This is a significant disadvantage in their characterization and plausible technological applications. A breakthrough was made by incorporating long flexible side chains to the conjugated backbone. Polythiophene and its 3-substituted derivatives represent one family of this kind of polymer, in which the substituents can be alkyl(R),[1,2] alkoxy(OR),[3,4] alkylthio(SR),[5,6] alkanesulfonic acid (RSO_3H)[7] or aromatic[8] groups. Among them, the electron-donating SR-substituted polythiophenes have attracted a lot of attention[5,6,9–11] because the electron-donating groups are expected to produce polythiophene derivatives with low band gaps through raising the energy level of the highest occupied orbital (HOMO). This decreases the oxidation potentials of these polymers, and consequently stabilizes their conducting states.[9]

Usually, a high degree of π-electron conjugation and a coplanar polymer backbone favor high conductivity when doped.[12] However, substituents like SR or R groups on the thiophene rings tend to cause a steric hindrance and, consequently, a lower degree of coplanarity along the polymer backbone as compared to the unsubstituted parent polymers.[12] Amongst the SR and R functional groups, because SR is more flexible than R, SR-functionalized polymers are expected to have higher coplanarity than their R-functionalized analogues, and thus a higher conductivity.

If singlet excitons are formed after semiconducting polymers are excited by photo- or electro-stimulation, the radiative decay of singlet excitons to the ground states of the polymers leads to light emission. The polymers able to realize these processes are fluorescent polymers. There are several ways to increase the electroluminescence efficiency through polymer structure modification, including incorporating non-conjugated fractions along the polymer backbone so that excitons are confined and the non-radiative decay of singlet excitons is suppressed;[13] modulating the positions of the band edges of the polymer through derivatization of the polymer backbone, for instance with electron-donating or -accepting groups, so that the energy barrier between the Fermi energy of the cathode (anode) and the energy of the frontier levels of the emissive polymers are reduced, and thus an efficient charge injection can be achieved;[13] increase of the torsional angle between the adjacent units so that a polymer backbone structure with shorter mean conjugation length is formed and relaxation from the excited state through non-radiative (e.g. thermal) processes is reduced.[14,15] Based on the above summary, SR-functionalized conjugated polymers are expected to have a lower bandgap energy, a higher conductivity and a lower fluorescence quantum yield as compared with their R-functionalized analogues.

During studies of SR-functionalized polythiophene derivatives, although the fluorescent properties of this kind of conducting polymers had been noted and reported,[6,11] only one report gave information about the quantum yield of this kind of polymer.[6] Our research group has ongoing interest in studying the structure-property correlation of conjugated polymers. It is noted that polymerization of monomers incorporating thiophenediyl and acetylene[16,17] has led to polymers showing very

Published on the web July 15, 2003; DOI 10.1246/bcsj.76.1449

good fluorescence due to the insertion of acetylene units, in addition to the attained structural regioregularity. We studied the synthesis and characterization of the polymers comprising alternating phenylene and alkyl-substituted thiophenediyl/bithiophenediyl repeating units (**P1′** and **P2′**, alkyl = butyl, octyl and dodecyl).[18–20] A higher fluorescence quantum yield and a blue shift in the emission wavelength were observed. We therefore designed and synthesized two series of polymers of similar structure incorporating phenylene and thiophenediyl/bithiophenediyl repeating units, but with alkylthio substituents replacing the alkyl side chains: **P1** and **P2**. The objective was to prepare new highly fluorescent polymers functionalized with SR groups and to further understand the structure-property correlation. The structures of polymers **P1** and **P2** as well as **P1′** and **P2′** are shown in Chart 1. The results indicate that the SR-functionalized polymers are highly fluorescent with quantum yields comparable to those of the R-functionalized analogues. The detailed influence of a structural modification by replacing R with SR on the polymer properties are reported and discussed in the following, compared with their R-functionalized analogues.

Results and Discussion

Physical Properties. **P1** and **P2** were synthesized by Grignard coupling and the $FeCl_3$ oxidation methods, respectively, as shown in Scheme 1. The syntheses of **P1** and **P2** were more difficult than their R-functionalized analogues, **P1′** and **P2′**, because of the replacing of R by SR. **P2** are brown or brownish green powders, which are partially soluble in CS_2, $CHCl_3$, THF and toluene. The solubility of **P2** polymers decreases with an increase in the alkylthio chain length. **P1a** is a dark-red powder, but **P1b** and **P1c** are dark-red sticky materials. They can be easily dissolved in the above-mentioned solvents. Films of **P1** evaporatively cast from toluene solution are transparent and smooth, but those of **P2** are not.

Table 1 summarizes the number-averaged molecular weights (M_n) of the polymers, as determined by GPC using polystyrene as a standard. The M_n for **P1a** is 3700, corresponding to about 30 aromatic units in a polymer chain. M_n for **P1b** and **P1c** are around 2900, indicating a lower degree of polymerization due to the lower reactivity of the monomers with an increase in the side chain length. M_n for **P2** is in the range of 2600–3000, contributed mainly by the lower molecular weight components, because the polymers are only very slightly soluble in THF. The insoluble part of the polymers is expected to have a higher molecular weight. The moderate molecular weights of the polymers are at the same order as those of the SR-functionalized polythiophenes prepared by different methods (R = ethylthio, bis(ethylthio) and ethylenedithio, M_n = 2200, 2600 and 3030/4750, respectively).[5,6,10,11]

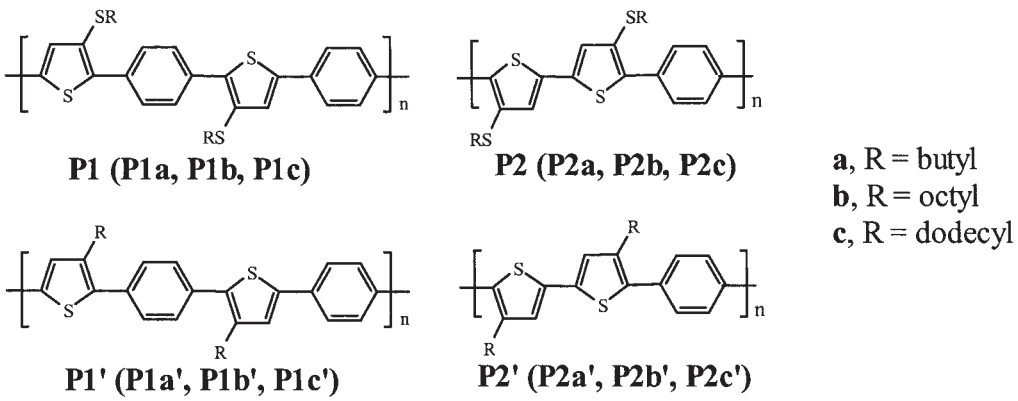

Chart 1. Polymer structure of **P1**: poly(3-alkylthio-2,5-thiophenediyl-1,4-phenylene-*alt*-4-alkylthio-2,5-thiophenediyl-1,4-phenylene) and **P2**: poly[4,4′-bis(alkylthio)-2,2′-bithiophene-5,5′-diyl-*alt*-1,4-phenylene].

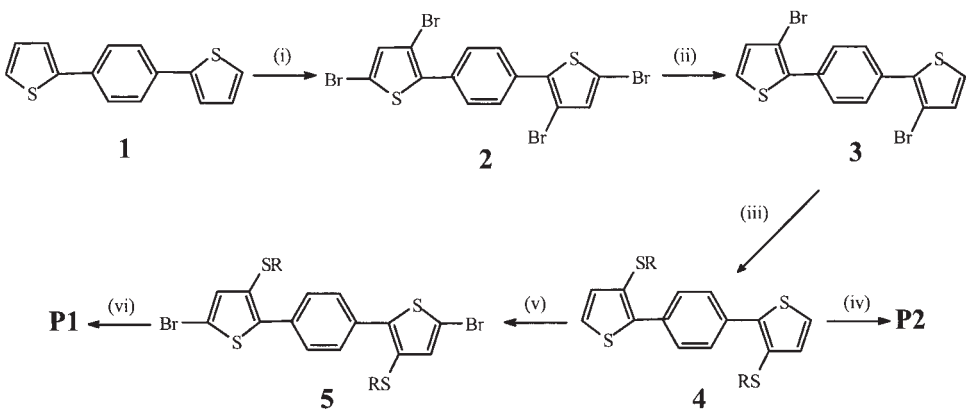

Scheme 1. Reagent and conditions: (i) 4 molar amounts bromine, AcOH/$CHCl_3$; (ii) zinc dust, 2-propanol; (iii) sodium 1-alkanethiolate, CuO, KI, DMSO; (iv) 4 molar amounts $FeCl_3$, $CHCl_3$; (v) 2 molar amounts bromine, AcOH/$CHCl_3$; (vi) (a) Mg, 1,2-dibromoethane, THF; (b) 1,4-dibromobenzene, Ni(dppp)Cl_2, THF.

Table 1. Summary of Molecular Weights (M_n), Polydispersity Indices (PDI) and Conductivities (σ) of **P1** and **P2**

Polymer	GPC results		σ/S cm^{-1} a)	
	M_n	PDI	doped by I_2	doped by $FeCl_3$
P1a	3700	2.1	5.0×10^{-4}	—b)
P1b	2900	1.5	—c)	—c)
P1c	3000	1.5	—c)	—c)
P2a	2800	1.6	1.7×10^{-5}	1.0×10^{-4}
P2b	2700	1.7	1.3×10^{-5}	—b)
P2c	2900	2.5	2.5×10^{-5}	1.0×10^{-3}
P1a′	3900	2.2	7.4×10^{-4}	1.0×10^{-3}
P2a′	6700	2.7	2.0×10^{-1}	1.1×10^{-3}

a) The insoluble part of the polymers were used in conductivity experiments as the soluble part is not enough. b) Samples are too brittle to be measured. c) Neutral polymers are sticky materials.

The polymers are conductive (the insoluble part of the polymers was used in conductivity experiments because the soluble part was insufficient) when doped by I_2 or $FeCl_3$, as shown in Table 1, accompanied by a color change from brown to black. An I_2 uptake up to 200 w/w% is possible in some cases. However, their conductivities are lower than those of the alkyl-functionalized polymers. The polymers are expected to be more conductive because their substituent, SR, is a stronger electron-donating group than R. The reason for this unexpected result is discussed later.

Table 2 gives the elemental analysis results for neutral and $FeCl_3$-doped polymers. It can be seen that the ratio of chlorine to iron is around 4:1 from microanalyses of $FeCl_3$-doped **P1** and **P2**, indicating the insertion of an anion in the form of $FeCl_4^-$. This is consistent with the previously reported results.[21–23] The ratios of $FeCl_4^-$ to S from microanalyses suggest that one $FeCl_4^-$ is roughly associated with one repeating unit (one repeating unit contains four S atoms in **P1** and **P2**) along the polymer chain. These values are higher than those of the R-functionalized analogues, **P1′** and **P2′**, in which one repeating unit corresponds to about 0.6 dopants (one repeating unit contains two S atoms in **P1′** and **P2′**). Residue bromine and chlorine elements were also detected in polymers **P1** and **P2**, obtained when the brominated monomers were not completely converted into Grignard reagents and when chlorination occurred during $FeCl_3$ oxidation, respectively. The ratio of aromatic rings to Br or Cl atoms was calculated and compiled in Table 2. However, as compared to their R-functionalized analogues, **P1a** and **P2a** do not display a significant difference in the ratios.

Structure Characterization. Figure 1 shows the ^{1}H NMR spectra of monomer 1,4-bis(3-butylthio-2-thienyl)benzene (**4a**), polymers **P1a** and **P2a**. Because of the structural similarity, the overall line shapes of the ^{1}H NMR spectra of **4a**, **P1a** and **P2a** are close to those of their R-functionalized analogues,[20] except that the resonances are mostly shifted downfield due to the replacement of R by SR. Thus, the assignment of the resonances is not given in detail here. The information from ^{1}H NMR spectra suggests that polymers **P1** and **P2** have the expected 2,3,5-trisubstituted thiophene units and 1,4-disubstituted benzene rings in their polymer backbone. The polymers were obtained as expected with regioregular structures, and no cross-linking occurred during polymerization. Moderate molecular weights for **P1** and **P2** are also suggested, because the two sets of doublets at δ 7.10 and 7.30 can be seen in the aromatic range, ascribable to the C_β-H and C_α-H resonances on the terminal thiophenediyl rings, respectively. In the FTIR spectra (not shown), regioregular polymer structures were also suggested, in agreement with the results from NMR studies. The existence of sulfur is indicated by strong C–S stretching at 627 cm^{-1}.[5]

UV-Vis Absorption and Fluorescence Spectra. Just like the polymers **P1′** and **P2′**, which are functionalized with alkyl groups, the polymers **P1** and **P2** are also highly fluorescent. They absorb light at around 400 nm, corresponding to their π–π^* transitions, but emit green light strongly at about 520 nm, which is discernible to the naked eye. The peak wavelengths, bandgaps and relative quantum yields with quinine sulfate as a reference, are summarized in Table 3. Those of **P1b′** and **P2b′** are included for a comparison. Because **P1** polymers can be

Table 2. Elemental Composition Determined from Microanalysis

Polymer	Expected elemental composition	Determined elemental composition	Ratio of aromatic units to Br or Cl atoms
P1a	$C_7H_7S_1$	$C_{6.01}H_{7.30}S_{1.00}Br_{0.05}$ a) $C_{6.17}H_{8.00}S_{1.00}Fe_{0.33}Cl_{1.18}$ b)	20:1
P1b	$C_9H_{11}S_1$	$C_{8.13}H_{13.02}S_{1.00}Br_{0.15}$ a)	6.7:1
P1c	$C_{44}H_{60}S_4$	—c)	
P2a	$C_{5.5}H_6S_1$	$C_{5.05}H_{5.47}S_{1.00}Cl_{0.02}$ a) $C_{5.57}H_{4.61}S_{1.00}Fe_{0.26}Cl_{0.96}$ b)	37.5:1
P2b	$C_{7.5}H_{10}S_1$	$C_{6.38}H_{10.65}S_{1.00}Cl_{0.04}$ a) $C_{6.52}H_{7.00}S_{1.00}Fe_{0.29}Cl_{1.00}$ b)	18.8:1
P2c	$C_{9.5}H_{14}S_1$	$C_{7.38}H_{10.50}S_{1.00}Cl_{0.08}$ a) $C_{7.11}H_{9.16}S_{1.00}Fe_{0.31}Cl_{0.98}$ b)	9.4:1
P1a′	$C_{14}H_{14}S_1$	$C_{12.60}H_{14.42}S_{1.00}Br_{0.08}$ a) $C_{13.04}H_{13.80}S_{1.00}Fe_{0.33}Cl_{1.46}$ b)	25:1
P2a′	$C_{11}H_{12}S_1$	$C_{11.70}H_{12.51}S_{1.00}Cl_{0.038}$ a) $C_{10.68}H_{13.86}S_{1.00}Fe_{0.28}Cl_{1.15}$ b)	39.4:1

a) Neutral polymers. b) Powder polymers chemically doped by $FeCl_3$. c) Not enough **P1c** to be measured.

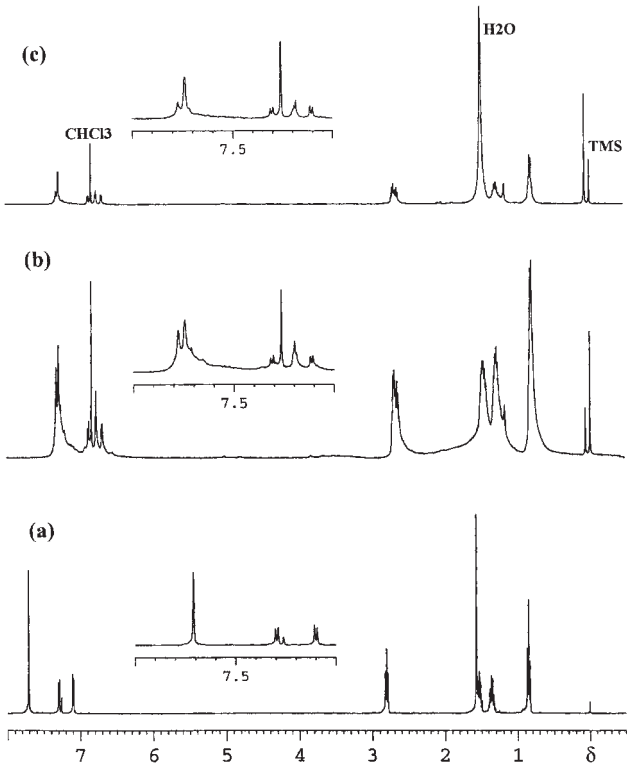

Fig. 1. ^{1}H NMR spectra of (a) **4a**, (b) **P1a**, (c) **P2a**.

Table 3. Summary of Results from Absorption and Emission Spectra of **P1** and **P2** Polymers in Solution and Solid States

Sample		λ_{max}/nm	λ_{em}/nm	Quantum yield/%[a)]	Optical bandgap/eV
$CHCl_3$ solution	**P1a**	400	510	25	
	P1b	396	510	33	
	P1c	396	510	23	
	P1b′	386	488	66	
	P2b′	398	494	23	
CS_2 solution	**P1a**	416	522	30	
	P1b	414	524	37	
	P1c	406	524	31	
	P2a	408	525	44	
	P2b	412	523	39	
	P2c	416	523	56	
film	**P1a**	410	530		2.37
	P1b	390	526		2.38
	P1c	390	526		2.34
	P1b′	388	512		2.64
	P2a	410	524		2.43
	P2b	420	524		2.40
	P2c	426	520		2.38
	P2b′	420	521		2.58

a) Relative to quinine sulfate in 0.1 M H_2SO_4.

dissolved in both $CHCl_3$ and CS_2 solvents and **P2** have higher solubility in CS_2 than in $CHCl_3$, the optical data obtained in $CHCl_3$ and CS_2 solutions are presented for the **P1** series, while those only in CS_2 are reported for the **P2** series. The solvent CS_2 seems to favor a more extended polymer conformation than $CHCl_3$, since both the λ_{max} and λ_{em} of **P1** polymers are red-shifted in CS_2 with reference to those in $CHCl_3$. The relative quantum yields of **P1** in CS_2 are all higher than those in $CHCl_3$.

It can be seen that replacing R with SR causes a slight red shift in the absorption and emission peak wavelengths. A lower bandgap of SR-substituted polymers than that of the R-substituted analogues is also observed, as expected.

The fluorescent quantum yields of **P1** and **P2** in the solution state are in the range of 23–56% relative to quinine sulfate, comparable to those of **P1′** and **P2′** (19–69%).[20] This is in contrast to the expectation that **P1** and **P2** should have a higher coplanarity along the polymer backbone than **P1′** and **P2′**, and thus a lower quantum yield, because SR is more flexible than R. The fluorescence quantum yield of poly(3-butylthio-2,5-thiophenediyl) in chloroform was reported to be greater than 0.01,[6] corresponding to a relative quantum yield of about $>$ 1.8% with reference to quinine sulfate. It is obvious that the current polymers incorporating phenylene and thiophenediyl/bithiophenediyl repeating units have higher quantum yields. This effect can be attributed to the phenylene moieties contributing to a more rigid polymer structure, with the effect that the relaxation from the excited state through the non-radiative (e.g. thermal) process would be reduced with consequently higher fluorescent quantum yields.[15,24]

Literature reports about the fluorescent characteristic of SR-functionalized poly(thiophene) derivatives are not as many as those of R- and OR-functionalized ones. To the best of our knowledge, only poly(3-butylthio-2,5-thiophenediyl),[6] poly(3,4-ethylenedithio-2,5-thiophenediyl)[11] and the copolymers incorporating alkylthiothiophenediyl and 4,4′-biphenylene repeating units were reported to be fluorescent.[25] The emission wavelength maxima (λ_{em}) of the former two polymers were located at 603 and 552 nm, respectively, in the solution state.[6,11] These are red shifted, as compared to those of **P1** and **P2** (510–520 nm) in solution. On the other hand, λ_{em} of the copolymers incorporating alkylthiothiophenediyl and 4,4′-biphenylene repeating units peaked at 485 nm in the film state,[25] which is blue shifted as compared to those of **P1** and **P2** (520–530 nm) films. These results suggest a trend: the insertion of phenylene units tends to make λ_{em} blue shifted and the more the phenylene units in the polymer backbone, the shorter the λ_{em} of the polymers. The bandgaps of **P1** and **P2** are in the range of 2.34 to 2.43 eV, in between those of ethylthio-, bis(ethylthio)-, ethylenedithio-substituted polythiophenes (2.0 to 2.24 eV)[11] and the polymer comprising 4,4′-biphenylene and 3-alkylthio-2,5-thiophenediyl units (2.57 eV).[25] This suggests that with the insertion of phenylene moieties, the polymer has a bigger torsional angle or shorter mean conjugation length along the polymer backbone, and consequently a higher bandgap energy.

Thermogravimetry (TG) and Modulated Differential Scanning Calorimetry (MDSC). The thermooxidative stability of functional polymers is an important property to consider in their applications as device materials. The thermal stability of **P1** and **P2** was examined by TG, in comparison with that of the R-functionalized polymers. Just as the R-

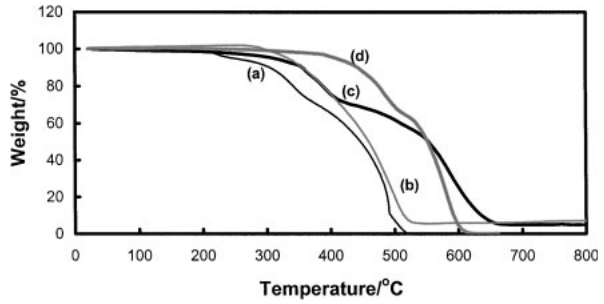

Fig. 2. TG plots of (a) **P2a**, (b) **P2a′**, (c) **P1a**, (d) **P1a′** in air.

substituted polymers reported in our previous work, polymers with shorter side chains are generally more thermally stable than those with longer chains. However, the decomposition behaviors of SR- and R-functionalized polymers are different. Figure 2 shows the TG thermograms of **P2a** (a), **P2a′** (b), **P1a** (c) and **P1a′** (d) in air. Two main decomposition steps are involved. The first is due to the cleavage of a substituent chain, the second to degradation of the polymer backbone. In the present series of polymers, the decomposition of the first step starts at significantly lower temperatures for the SR-functionalized polymers (thermogram a), as compared to the corresponding R-substituted ones (thermogram b). A possible reason is that the thio etheral linkages between the alkyl group and thiophenediyl rings are weak sites susceptible to thermooxidative attack. The difference in bond energies of C–C (317 KJ/mol) and C–S (290 KJ/mol) may serve as a support to this prediction.[26] Interestingly, the order of stability of **P1a** (thermogram c) and **P1a′** (thermogram d) reversed above 550 °C. It was reported that sulfur-containing compounds might undergo pyrolysis to produce sulfur-containing radicals, ArS$^{\bullet}$, which could dimerize to afford additional compounds, such as ArSSAr, or couple with Ar$^{\bullet}$ to form ArSAr.[27] These cross-linking reactions can lead to the formation of pseudo-ladder polymers that may be responsible for the high thermal stability of **P1a** over **P1a′** at high temperatures. In addition, the thermal stability of **P1a** (thermogram c) is better than that of **P2a** (thermogram a), in parallel with the superior thermal stability of **P1a′** (thermogram d) to that of **P2a′** (thermogram b).

MDSC[20] was employed to study the technologically important glass-to-rubber transition of the current series of polymers. Well-defined glass transitions of the polymers were observed, the results are summarized in Table 4. T_g(s) for the **P1′** and **P2′** series are also included for a comparison. The results show that in both series of polymers the introduction of a long side chain (going from butyl, octyl to dodecyl) lowers T_g significantly. This can be understood because the onset of the glass transition is associated with the start of rotation of the C–C bonds along the polymer backbone. The long side chains push the neighboring polymer chains away, hence reducing the intermolecular attraction, acting as an internal lubricant, or plasticizer. For the **P1** series, the SR substituent significantly lowers T_g compared to the R analogues, but the opposite is observed for the **P2** series, although the difference is much smaller. The results also clearly indicate that the **P2′** and **P2** series have much higher T_gs than their **P1′** and **P1** analogues. This is due to the greater steric hindrance exerted by the pendant groups, which are in closer proximity in the former series.

Table 4. Glass Transition Temperatures (T_g) of **P1**, **P2** and Their R-Functionalized Analogues **P1′** and **P2′** as Determined from MDSC

Polymer	T_g/°C	Polymer	T_g/°C
P1a	26.4	**P1a′**	58.3
P1b	−38.8	**P1b′**	−4.0
P1c	—[a)]	**P1c′**	−19.2
P2a	129.0	**P2a′**	122.3
P2b	55.3	**P2b′**	50.4
P2c	65.4	**P2c′**	59.6

a) Polymer is too little to be measured.

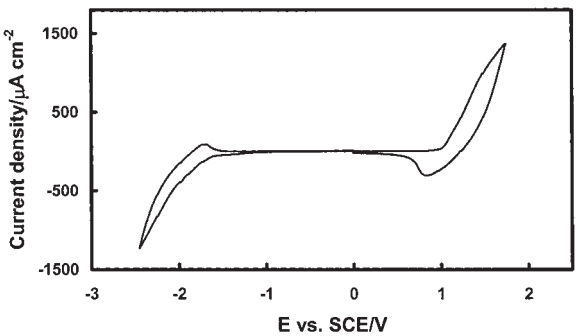

Fig. 3. CV curve of **P1a**. The scan rate is 50 mV s^{-1}.

Cyclic Voltammetry. The electrochemistry of toluene cast films of the **P1** and **P2** polymers was investigated using cyclic voltammetry (CV) in a 1 M acetonitrile solution of Bu_4NBF_4. **P1** polymers are all concurrently *p*- and *n*-dopable, accompanied by a color change from yellow to black and blue, respectively. The CV curves at both anodic (*p*-doping) and cathodic (*n*-doping) directions obtained for **P1a** are shown in Fig. 3. The limited reversibility of the oxidation and reduction processes is shown in both anodic and cathodic sweeps, probably due to degradation of the polymers. Repeated scanning or scanning to a wider potential range deactivated the film. Nevertheless, the reversibility and stability were good at moderate oxidation or reduction potentials.

For **P2** films, the occurrence of *n*-doping was accompanied by a very sharp color change from brown to blue or greenish-blue, although no well-defined onset or peak potential was observed in their CV profiles. This was because the *n*-doped **P2** polymers were very easily soluble in acetonitrile. In addition, a very serious "break-in" phenomenon[28] was observed during cathodic scanning due to the poor quality of the films. However, no color change was observed in the poorly defined *p*-doping process.

Table 5 summarizes the onset and peak potentials for both the *p*- and *n*-doping processes of the **P1** polymers. Those of **P1a′** are also included for a comparison. Bandgaps evaluated as the difference of the onset potentials of the two processes are also listed. With an increase in the side chain length, both the *p*- and *n*-doping onset potentials increase, resulting in almost unchanged bandgaps. In addition, the electrochemical bandgaps are about 0.3 eV higher than the optical ones (Table 2), as observed and discussed earlier.[20]

Table 5. Summary of CV Results

Polymer	*p*-doping			*n*-doping			E_g/eV
	E_{on}/V	E_{pa}/V	E_{pc}/V	E_{on}/V	E_{pa}/V	E_{pc}/V	
P1a	1.01	1.42	0.84	−1.59	—[c]	−1.71	2.60
P1b[a]	1.11	1.72	—[c]	−1.50	—[c]	−1.67	2.61
P1c[a,b]	1.23	1.61	—[c]	−1.34	−1.78	—[c]	2.57
P1a′	1.05	1.33	0.60	−1.87	−2.14	−1.88	2.92

a) Degradation occurred in both *p*- and *n*-doping processes. b) Film peeled from electrode surface and some of the readings may be unreliable. c) Unresolved.

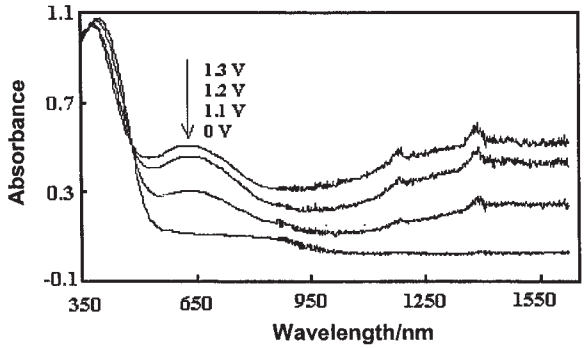

Fig. 4. In situ potential dependent UV-Vis-NIR spectra of **P1a** during *p*-doping process.

In comparison with **P1a′**, the electrochemical bandgap of **P1a** is smaller by 0.32 eV. This is in accordance with the trend obtained in optical bandgaps. However, an analysis of the onset potentials of its *p*- and *n*-doping processes shows that this reduction is mainly contributed by an increase in *n*-type onset potential, although a minor decrease is also observed in the onset potential of the *p*-doping process. This does not agree very well with the prediction that the stronger electron-donating ability of the SR group should greatly raise the energy level of the valence band, i.e., to lower the onset potential of *p*-doping. We had attempted to find a possible reason, for instance, the residue electron-withdrawing Br- or Cl-substituent on the polymer backbone might be responsible for the observation. However, the ratios of the aromatic rings to Br or Cl atoms in the polymer chains of **P1a** and **P2a** are not significantly lower than those of **P1a′** and **P2a′** (Table 2), thus excluding this possibility.

Electrochromism. The change in the UV-Vis-NIR spectra during electrochemical oxidation or reduction provides direct evidence for the doping processes, and gives information about the electronic band structure of the polymers. Figure 4 shows the UV-Vis-NIR spectra of **P1a** upon *p*-doping. When the applied potential is higher than its onset value, the color of the film changes from brown to black, and two new broad absorption bands emerge at 630 nm and about 1600 nm. Increasing the potential causes an increase in the intensity of the bands, together with a slight blue shift in the bandgap and a slight decrease in the intensity of the π–π* transition. These features of optical transitions are due to the formation of bipolarons.[9–11]

The *n*-dopability of the polymer films was also directly shown by the spectral change measured in situ when cathodic

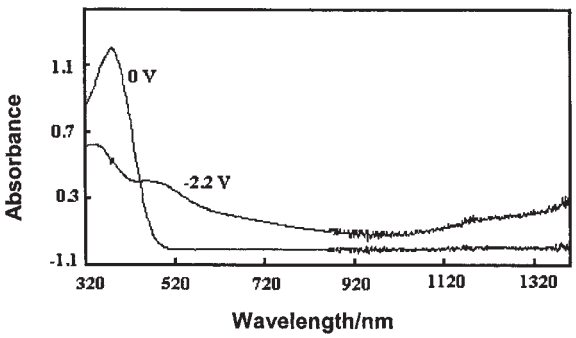

Fig. 5. In situ potential dependent UV-Vis-NIR spectra of **P1a** during *n*-doping process.

potentials were applied, as shown in Fig. 5 for **P1a**. Two new broad bands at 460 nm and > 1400 nm, which are different from those in *p*-doping (Fig. 4), were observed when reduced at −2.2 V accompanied by the color change from brown to blue. A dramatic spectral change (not shown) was also observed when a cathodic potential (e.g., −2.2 V) was applied to **P2** polymers, although the doped polymers dissolved in the solvent easily.

XPS. XPS has been used to study the different electronic environments experienced by different atoms, and to calculate the doping level in the present polymers. Figure 6(a) and (b) show the S(2p) core level spectra of **P2b** in the neutral and $FeCl_3$-doped states, respectively. The S(2p) spectrum deconvolution for the neutral polymer involves two spin-orbit splitting doublets [$S(2p_{3/2})$ and $S(2p_{1/2})$, $\Delta E = 1.2$ eV, area ratio = 2:1], with BE of $S(2p_{3/2})$ peaks at 163.1 and 164.0 eV, respectively. The two different environments have been assigned to the sulfur atoms on the alkylthio side chain (S_a) and on the thiophenediyl ring (S_r),[29] respectively. When the polymers are doped, four chemical environments are best deconvoluted from the S(2p) envelope. The $S(2p_{3/2})$ binding energies for the four S species are at 163.1, 164.0, 165.1 and 166.7 eV, respectively. While the first two environments are attributed to the neutral sulfur atoms on the alkylthio group and thiophenediyl ring, the BE at 165.1 eV is probably associated with the ring sulfur species, which is positively charged due to the oxidation by $FeCl_3$[30] (denoted as S_r^+). The tailoring part with its $S(2p_{3/2})$ component possessing the highest BE at 166.7 eV is due to the oxidation of S atoms on the side chain into sulfone groups.[29]

Thus, the doublets with BE of $S(2p_{3/2})$ at 163.1 and 166.7 eV are assigned to the neutral and sulfone species, which locate on the substituent group. However, their (S_a) sum constituents about only 39% of the total sulfur (Table 6). This suggests that some of the S_a may be involved in other environments, in order to account for the theoretical 50% of the S_a in total sulfur. A possible explanation had been put forward by other researchers.[10,31,32] Based on results obtained from conductivity and absorption spectrum changes before and after doping, they suggested the oxidation of pendant sulfur and oxygen atoms into positively charged species by the dopants. Our observation here can serve as direct evidence from the viewpoint of XPS for the oxidation of sulfur atoms located on the pendent chains.

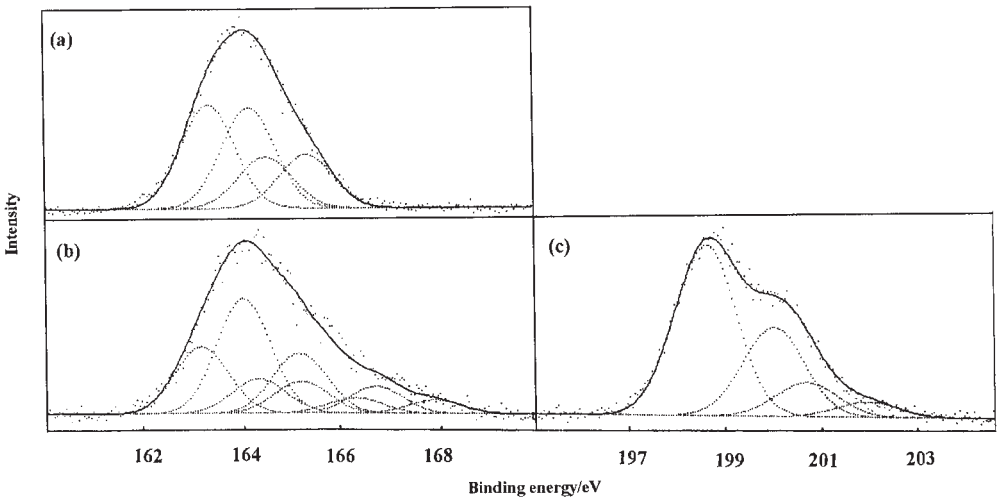

Fig. 6. XPS spectra of **P2b**: (a) S(2p) spectrum of neutral polymer; (b) S(2p) spectra of $FeCl_3$-doped polymer; (c) Cl(2p) spectra of $FeCl_3$-doped polymer.

Table 6. Summary of Results Relevant to Doping Level from XPS Analysis

Polymer[a)]	$[Cl\text{-}Cl_c]_4/[S]/\%$[b)]	$[S_a]/[S]/\%$[c)]	$[S_a^+]/[S_a]/\%$[d)]
P1a	8	47	6
P1b	9	48	4
P1c	5	49	2
P2a	29	39	22
P2b	30	39	22
P2c	49	29	42

a) Samples are doped by $FeCl_3$. **P2** are in powder form but **P1** are films. b) The value of $[Cl\text{-}Cl_c]_4/[S]$ indicates the normalized amount (in percentage) of charged chlorine species (Cl^-) corresponding to the total sulfur. Hence, 4 times of this value affords the average number of dopants associated with one monomeric repeating unit, as the latter contains 4 sulfur atoms. c) Low value of $[S_a]/[S]$ means that large percentage of S_a are positively charged or the corresponding doping level is high; on the contrary, high value indicates a low doping level. This is reflected in the next column, the correponding $[S_a^+]/[S_a]$. d) $[S_a^+]/[S_a] = 2 \times (50\% - [S_a]/[S])$. It is the percentage of the positively charged S_a in the total S_a.

The Cl(2p) spectrum is presented in Fig. 6(c). As reported earlier,[20] the two doublets are attributed to the chlorine species involved in the dopant ($FeCl_4^-$) and the C–Cl bond[30] (denoted as Cl_c), respectively. $[Cl\text{-}Cl_c]_4/[S]$ can also serve as a measure of the doping level (Table 6). These results are in good agreement with those obtained by elemental analysis (Table 2).[20] **P1** films have lower values of $[Cl\text{-}Cl_c]_4/[S]$ and $[S_a^+]/[S_a]$, compared with those of **P2**. This is because the **P1** samples are in the film state, which can be dedoped easily.

Stability of the Doped States. The I_2-doped **P2′** were easily dedoped when the compressed pellets were ground into powder.[20] The dedoping resulted in the regeneration of undoped polymers, as indicated by TG and FTIR spectral data. However, the I_2-doped SR-substituted polymers are more stable and the FTIR spectra (not shown) of I_2-doped samples show strong doping-induced features, as reported for poly(3,4-ethylenedithio-2,5-thiophenediyl).[11] The I_2-doped state is thermally stable, because a thermal treatment of I_2-doped **P2** at 100 °C for 24 h showed no intensity decrease in the FTIR spectrum. However, the high doping level (I_2 weight uptake $\sim$ 200 w/w% for **P2** vs $\sim$ 120 w/w% for **P2′**[18]) and good thermal stability did not make the **P2** polymers more conductive, since their conductivities are mostly in the range of 10^{-4}–10^{-5} S cm^{-1} (Table 1).

In view of the high doping level indicated by the results from elemental analyses, XPS and I_2 weight uptake, the low conductivities of the I_2- and $FeCl_3$-doped **P2** series of polymers are unexpected. The low conductivities together with the high thermal stability of the doped states, especially when doped by I_2, seem to suggest that the bipolarons formed upon doping are partially localized. This is in line with the XPS result mentioned above, which suggests the presence of positively charged sulfur atoms on the pendant alkylthio side chains.

Conclusions

Two series of polymers comprising alkylthio (SR)-functionalized thiophenediyl/bithiophenediyl and phenylene units had been synthesized and characterized. They are highly fluorescent with emission located in the bluish green and green range in solution and film states, respectively. The results, together with those from literature reports, indicate that the insertion of phenylene units is an efficient way to tune the emission color and to increase the fluorescence quantum yield of conjugated polymers. As compared to the alkyl(R)-functionalized analogues, the SR-functionalized polymers have lower bandgap energies through raising the reduction onset potentials and comparative fluorescence quantum yields. This may imply that replacing of R by SR did not bring higher coplanarity to the polymer backbone, and the electronic effect of the SR group was thus not effectively displayed. The doping levels of the chemically oxidized SR-functionalized polymers are high, as suggested by microanalysis and XPS results, but this did not make them highly conductive. The oxidation of the sulfur atoms on the SR side chains and, consequently, the

localization of polarons and bipolarons may be responsible for the observation.

Experimental

Materials. Tetrahydrofuran (THF), dimethyl sulfoxide (DMSO) and acetonitrile were carefully dried before use. 2-Bromothiophene, 1,4-dibromobenzene, bis(diphenylphosphino)nickel dichloride [Ni(dppp)Cl_2], 1-butanethiol, 1-octanethiol and 1-dodecanethiol were used as received. 1,4-Bis(2-thienyl)benzene (**1**) was synthesized in a similar way as for 1,4-bis(3-alkyl-2-thienyl)benzene[20] using 2-bromothiophene and 1,4-dibromobenzene as starting materials.

Instrumentation. ^{1}H NMR spectra were recorded on a 300 MHz Bruker ACF 300 FT-NMR spectrophotometer. 75 MHz ^{13}C NMR spectra were obtained using the same instrument. Deuterated chloroform was used as a solvent and tetramethylsilane (TMS) as an internal reference. EIMS and HRMS spectra were obtained using a micromass 7034E Mass Spectrometer. Elemental analyses of all the monomers and polymers were conducted at the NUS Microanalytical Laboratory on a Perkin-Elmer 240C elemental analyzer for C, H, and S determination. Halogen determination was made by either ion chromatography or the oxygen flask method. Gel permeation chromatography (GPC) analyses were carried out using a Perkin Elmer Model 200 HPLC system with Phenogel^{TM} MXL and MXM columns (300 mm $\times$ 4.6 mm ID, MW 100–100K and 5K–500K, respectively) calibrated using polystyrene standards. THF was used as an eluent, and the flow rate was 0.35 mL min^{-1}. The FTIR spectra of the polymers and monomers dispersed in KBr disk was recorded on a Bio-Red TFS 156 spectrometer. Solution phase and solid state (films were evaporatively cast from toluene solution) absorption and fluorescence spectrum measurements of the polymers were conducted on a Hewlett Packard 8452A spectrophotometer and Shimadzu RF5000 fluorescence spectrophotometer, respectively. Thermogravimetry (TG) was conducted on a Du Pont Thermal Analyst 2100 system with a TGA 2950 thermogravimetric analyzer in air (75 mL min^{-1}) at a heating rate of 10 °C min^{-1} from room temperature to 1000 °C. Modulated differential scanning calorimetry (MDSC) was conducted on a TA Instruments 2910 differential scanning calorimeter upgraded with an MDSC^{TM} option in N_2 (70 mL min^{-1}) using a heating rate of 1 or 2 °C min^{-1}, an oscillation amplitude of 1 or 2 °C, respectively, and an oscillation period of 60 or 80 s from -100 to 170 °C unless otherwise stated. Conductivity measurements were carried out on polymer pellets of known thickness using a four-point probe connected to a Keithley constant current source. XPS measurements of polymer powder or films (on ITO) were performed by means of a VG ESCA/SIMLAB MKII with a Mg Kα radiation source (1253.6 eV). The binding energies were corrected for surface charging by referencing to the designated hydrocarbon C(1s) binding energy as 284.6 eV.

Cyclic voltammetry of solution cast polymer films was carried out using an EG&G 273A potentiostat/galvanostat controlled by EG&G M270 research electrochemistry software under an argon atmosphere at a scan rate of 50 mV s^{-1}. A three-electrode single-compartment chemical cell consisting of an ITO glass plate as the working-electrode, a platinum wire as the counter electrode, an $Ag/AgNO_3$ (0.1 M, in acetonitrile) (1 M = 1 mol dm^{-3}) as the quasi-reference electrode [0.35 V versus a saturated calomel electrode (SCE)] and a solution of 1 M Bu_4NBF_4 in acetonitrile as electrolyte was employed. In situ electrochromism studies of polymers were conducted in a single-compartment, three electrode quartz cell comprising a film-coated ITO working-electrode, a platinum counter electrode and a silver wire quasi-reference electrode using the potentiostat together with a Lamda 900 UV-Vis-NIR spectrometer in the same electrolyte system as CV.

Synthesis. The general schematic synthesis routes to the polymers are shown in Scheme 1. The main monomers employed were 1,4-bis(3-alkylthio-2-thienyl)benzene (**4**, alkyl = butyl, octyl and dodecyl). While **P1** polymers were prepared by polycondensation of the Grignard reagents of the dibromination product of **4** with 1,4-dibromobenzene, **P2** polymers were made by the chemical oxidation of **4** using $FeCl_3$ as an oxidant.

1,4-Bis(3,5-dibromo-2-thienyl)benzene (2): **1** (2.42 g, 10.0 mmol) was dissolved in $CHCl_3$–AcOH (30 mL, 2:1) in a round-bottom flask, and bromine (3.32 g, 20.7 mmol) dissolved in the mixture solvent was added dropwise. The second portion of bromine (3.32 g, 20.7 mmol) was then added and stirred at room temperature for a few hours. The reaction mixture was refluxed at 60 °C overnight and then cooled to room temperature. It was extracted with $CHCl_3$ and washed by capacious water, sodium carbonate, water, dried and the solvent removed. Recrystallization from $CHCl_3$–EtOH yielded a needle-form solid. Yield: 5.2 g (94%); mp 201–202 °C. MS (EI, *m*/*e*, % intensity): 554 (M, 64), 556 (M + 2, 95), 558 (M + 4, 100), 560 (M + 6, 96), 562 (M + 8, 68). HR-MS Calcd for $C_{14}H_6S_2Br_4$ (M + 4): 557.6603, Found 557.6629. IR (cm^{-1}): 3096, 3040, 3017, 1625, 1541, 1489, 1437, 1404, 1304, 837, 804, 611, 476. ^{1}H NMR: δ 7.65 (4H, s), 7.04 (2H, s). ^{13}C NMR: δ 138.94, 133.85, 132.13, 128.84, 112.08, 107.02. Anal. Calcd for $C_{14}H_6S_2Br_4$: C, 30.11; H, 1.07; S, 11.47; Br, 57.35%. Found: C, 29.84; H, 1.22; S, 11.29; Br, 57.35%.

1,4-Bis(3-bromo-2-thienyl)benzene (3): **2** (9.70 g, 17.4 mmol) was mixed with a solution of 2-propanol (150 mL), AcOH (10 mL), water (2.8 mL) and concentrated HCl (0.6 mL). The mixture was refluxed and stirred vigorously when zinc dust (5.48 g, 83.8 mmol) was added in small portions until the selective reduction of **2** to **3** was completed. TLC (hexane as the eluent) was employed to monitor the progress of the reduction, by which R_f values of 0.64 were found for the starting material, 0.55 for the intermediate tribromo-substituted compound and 0.45 for the product. The reaction was completed and terminated by cooling to room temperature about 8 h later, as indicated by the disappearance of the first and the second points in TLC. The solvent was removed by a rotavapor and the residue extracted with ether. The ether layer was washed with water, dried, filtered and the solvent removed. Recrystallization from ethanol afforded the titled product. Yield: 3.55 g (51%); mp 119–120 °C. MS (EI, *m*/*e*, % intensity): 398 (M, 60), 400 (M + 2, 100), 402 (M + 4, 69). HR-MS Calcd for $C_{14}H_8S_2Br_2$ (M + 2): 399.8414, Found 399.8389. IR (cm^{-1}): 3102, 3067, 3021, 1605, 1543, 1487, 1433, 1406, 1342, 870, 835, 696, 611. ^{1}H NMR: δ 7.73 (4H, s), 7.31 (2H, d, J = 5.3 Hz), 7.07 (2H, d, J = 5.3 Hz). ^{13}C NMR: δ 137.43, 132.59, 131.82, 128.89, 125.18, 107.73. Anal. Calcd for $C_{14}H_8S_2Br_2$: C, 42.00; H, 2.00; S, 16.00; Br, 40.00%. Found: C, 41.63; H, 1.98; S, 16.31; Br, 40.28%.

General Procedure for the Preparation of 1,4-Bis(3-alkylthio-2-thienyl)benzene (4). In a 250 mL two-neck flask, sodium hydride (NaH, 60% dispersion in hexane, 0.96 g, 24 mmol) was washed with dry hexane and blown with N_2 to remove hexane. DMSO (7 mL) was then added, followed by the addition of 1-alkanethiol (24 mmol) dropwise. When the evolution of hydrogen ceased, **3** (2.4 g, 6.0 mmol) and a mixture of CuO (0.096 g, 1.2 mmol) and KI (0.096 g, 0.58 mmol) in DMSO (4 mL) were

transferred. The mixture was refluxed at 120 °C for 24 h under nitrogen and then cooled down, filtered and washed with $CHCl_3$. The filtrate was extracted with $CHCl_3$ and thoroughly washed with water. Drying, filtering and removing $CHCl_3$ led to a dark oily residue. It was doubly isolated by silica-gel chromatography using hexane–$CHCl_3$ (5:1) as the eluent, and collected as the product.

1,4-Bis(3-butylthio-2-thienyl)benzene (4a): Yield: 82%; mp 42–43 °C. MS (EI, *m/e*, % intensity): 418 (M^+, 100). HR-MS Calcd for $C_{22}H_{26}S_4$: 418.0917, Found 418.0912. IR (cm^{-1}): 3098, 3044, 3013, 2955, 2926, 2868, 1527, 1470, 1460, 1431, 1377, 885, 831, 723, 630. ^{1}H NMR: δ 7.71 (4H, s), 7.29 (2H, d, $J = 5.3$ Hz), 7.10 (2H, d, $J = 5.2$ Hz), 2.81 (4H, t, $J = 7.2$ Hz), 1.53 (4H, m), 1.30 (4H, m), 0.85 (6H, t, $J = 7.3$ Hz). ^{13}C NMR: δ 140.33, 133.03, 131.23, 128.86, 128.17, 124.02, 35.25, 31.41, 21.69, 13.51. Anal. Calcd for $C_{22}H_{26}S_4$: C, 63.16; H, 6.22; S, 30.62%. Found: C, 62.86; H, 6.26; S, 30.15%.

1,4-Bis(3-octylthio-2-thienyl)benzene (4b): Yield: 74%; mp 40–41 °C. MS (EI, *m/e*, % intensity): 530 (M^+, 38), 43 ($C_3H_7^+$, 100). HR-MS Calcd for $C_{30}H_{42}S_4$: 530.2169, Found 530.2178. IR (cm^{-1}): 3096, 3042, 3013, 2955, 2924, 2870, 1526, 1483, 1466, 1433, 1377, 881, 837, 717, 627. ^{1}H NMR: δ 7.71 (4H, s), 7.29 (2H, d, $J = 5.2$ Hz), 7.09 (2H, d, $J = 5.3$ Hz), 2.80 (4H, t, $J = 7.2$ Hz), 1.53 (4H, m), 1.21 (20H, m), 0.85 (6H, t, $J = 6.8$ Hz). ^{13}C NMR: δ 140.37, 133.05, 131.28, 128.85, 128.21, 123.96, 35.60, 31.66, 29.34, 29.01, 28.56, 22.50, 13.95. Anal. Calcd for $C_{30}H_{42}S_4$: C, 67.92; H, 7.92; S, 24.15%. Found: C, 67.59; H, 7.48; S, 24.49%.

1,4-Bis(3-dodecylthio-2-thienyl)benzene (4c): Yield: 75%; mp 44–45 °C. MS (EI, *m/e*, % intensity): 642 (M^+, 100). HR-MS Calcd for $C_{38}H_{58}S_4$: 642.3421, Found 642.3415. IR (cm^{-1}): 3096, 3044, 3011, 2955, 2922, 2851, 1524, 1483, 1466, 1430, 1377, 883, 837, 719, 627. ^{1}H NMR: δ 7.71 (4H, s), 7.29 (2H, d, $J = 5.2$ Hz), 7.09 (2H, d, $J = 5.3$ Hz), 2.80 (4H, t, $J = 7.2$ Hz), 1.54 (4H, m), 1.23 (36H, m), 0.88 (6H, t, $J = 6.7$ Hz). ^{13}C NMR: δ 140.33, 133.04, 131.26, 128.86, 128.19, 123.99, 35.60, 31.82, 29.55, 29.50, 29.40, 29.35, 29.25, 29.07, 28.58, 22.60, 14.03.

General Procedure for the Preparation of 1,4-Bis(5-bromo-3-alkylthio-2-thienyl)benzene (5). **4** (1.4 mmol) was dissolved in $CHCl_3$ (10 mL) in a two-neck round-bottom flask and bromine (0.46 g, 2.9 mmol) in AcOH (60 mL) was run in dropwise. The mixture was stirred at 40–50 °C for 24 h, cooled down and dried. After filtering and removing the solvent, a dark-brown oil was obtained. It was isolated by flash chromatography (hexane as the eluent) to offer a product that solidified at room temperature.

1,4-Bis(5-bromo-3-butylthio-2-thienyl)benzene (5a): Yield: 85%; mp 67–68 °C. MS (EI, *m/e*, % intensity): 574 (M, 89), 576 (M + 2, 100), 578 (M + 4, 93). HR-MS Calcd for $C_{22}H_{24}S_4Br_2$ (M + 2): 575.9109, Found 575.9187. IR (cm^{-1}): 3040, 3013, 2953, 2922, 2866, 1529, 1483, 1462, 1419, 1369, 870, 819, 735, 625, 476. ^{1}H NMR: δ 7.62 (4H, s), 7.04 (2H, s), 2.78 (4H, t, $J = 7.3$ Hz), 1.52 (4H, m), 1.35 (4H, m), 0.85 (6H, t, $J = 7.2$ Hz). ^{13}C NMR: δ 141.66, 133.36, 132.47, 128.98, 128.81, 110.87, 35.38, 31.33, 21.65, 13.48. Anal. Calcd for $C_{22}H_{24}S_4Br_2$: C, 45.83; H, 4.17; S, 22.22; Br, 27.78%. Found: C, 45.94; H, 4.61; S, 22.33; Br, 27.28%.

1,4-Bis(5-bromo-3-octylthio-2-thienyl)benzene (5b): Yield: 90%; mp 59–60 °C. MS (EI, *m/e*, % intensity): 686 (M^+, 34), 688 (M + 2, 63), 690 (M + 4, 50), 43 ($C_3H_7^+$, 100). HR-MS Calcd for $C_{30}H_{40}S_4Br_2$ (M + 2): 688.0182, Found 688.0204. IR (cm^{-1}): 3038, 3015, 2955, 2928, 2851, 1524, 1491, 1460, 1423, 1377, 870, 819, 731, 623, 459. ^{1}H NMR: δ 7.62 (4H, s), 7.04 (2H, s), 2.77 (4H, t, $J = 7.3$ Hz), 1.53 (4H, m), 1.28 (20H, m), 0.86 (6H, t, $J = 6.7$ Hz). ^{13}C NMR: δ 141.61, 133.33, 132.46, 128.97, 128.79, 110.87, 35.69, 31.68, 29.25, 29.04, 28.97, 28.52, 22.54, 14.00. Anal. Calcd for $C_{30}H_{40}S_4Br_2$: C, 52.33; H, 5.81; S, 18.60; Br, 23.26%. Found: C, 51.97; H, 5.87; S, 18.04; Br, 23.35%.

1,4-Bis(5-bromo-3-dodecylthio-2-thienyl)benzene (5c): Yield: 82%; mp 64–65 °C. MS (EI, *m/e*, % intensity): 798 (M^+, 36), 800 (M + 2, 54), 802 (M + 4, 50), 43 ($C_3H_7^+$, 100). HR-MS (peak match method) Calcd for $C_{38}H_{56}S_4Br_2$: 798.1631, Found 798.1626. IR (cm^{-1}): 3042, 3011, 2955, 2917, 2849, 1526, 1493, 1470, 1425, 1377, 870, 819, 717, 621, 461. ^{1}H NMR: δ 7.62 (4H, s), 7.04 (2H, s), 2.77 (4H, t, $J = 7.2$ Hz), 1.54 (4H, m), 1.23 (36H, m), 0.87 (6H, t, $J = 6.6$ Hz). ^{13}C NMR: δ 141.68, 133.37, 132.47, 128.96, 128.80, 110.85, 35.71, 31.81, 30.24, 29.54, 29.48, 29.25, 29.01, 28.50, 22.59, 14.02. Anal. Calcd for $C_{38}H_{56}S_4Br_2$: C, 57.00; H, 7.00; S, 16.00; Br, 20.00%. Found: C, 56.76; H, 6.65; S, 15.74; Br, 19.43%.

General Procedure for the Synthesis of Poly(3-alkylthio-2,5-thiophenediyl-1,4-phenylene-*alt*-4-alkylthio-2,5-thiophenediyl-1,4-phenylene) (P1). A solution of **5** (1.0 mmol) in THF (2 mL) was introduced into a round-bottom flask containing Mg (0.060 g, 2.5 mmol) and THF (0.5 mL). The mixture was stirred vigorously and refluxed under N_2 for 2 h, while 1,2-dibromoethane (70 μL, 0.84 mmol) was added in portions as an initiator. The reaction mixture was cooled down and a solution of 1,4-dibromobenzene (0.236 g, 1.00 mmol) and Ni(dppp)Cl_2 (10.8 mg, 0.0200 mmol) in THF (2 mL) was then transferred at 0 °C. The mixture was then warmed up to room temperature and refluxed for 24 h before being terminated by cooling down and pouring into methanol. A brown sticky material was obtained which was subjected to Soxhlet washing with acetone for 2 h.

Poly(3-butylthio-2,5-thiophenediyl-1,4-phenylene-*alt*-4-butylthio-2,5-thiophenediyl-1,4-phenylene) (P1a): Dark red powder. Yield: 57%. ^{1}H NMR: δ 7.74 (4H, m), 7.64 (m), 7.30 (d, $J = 5.2$ Hz), 7.19 (1H, m), 7.10 (d, $J = 5.2$ Hz), 2.82 (2H, m), 1.56 (2H, m), 1.37 (2H, m), 0.85 (3H, m). ^{13}C NMR: δ 134.77, 132.82, 131.25, 128.72, 127.60, 124.12, 35.32, 31.41, 21.72, 13.54. Anal. Calcd for $C_{14}H_{14}S_2$: C, 68.29; H, 5.69; S, 26.02; Br, 0%. Found: C, 63.72; H, 6.11; S, 27.22; Br, 4.01%.

Poly(3-octylthio-2,5-thiophenediyl-1,4-phenylene-*alt*-4-octylthio-2,5-thiophenediyl-1,4-phenylene) (P1b): Red sticky material. Yield: 50%. ^{1}H NMR: δ 7.74 (4H, m), 7.62 (m), 7.29 (m), 7.19 (1H, m), 7.10 (m), 7.03 (m), 2.83 (2H, m), 1.56 (2H, m), 1.23 (10H, m), 0.86 (3H, m). ^{13}C NMR: δ 134.84, 132.82, 131.30, 128.71, 127.66, 124.08, 35.68, 31.71, 29.34, 29.04, 28.60, 22.55, 14.00. Anal. Calcd for $C_{18}H_{22}S_2$: C, 71.52; H, 7.28; S, 21.19; Br, 0%. Found: C, 62.21; H, 8.12; S, 19.91; Br, 6.43%.

Poly(3-dodecylthio-2,5-thiophenediyl-1,4-phenylene-*alt*-4-dodecylthio-2,5-thiophenediyl-1,4-phenylene) (P1c): Red sticky material. Yield: 10%. ^{1}H NMR: δ 7.73 (4H, m), 7.61 (m), 7.30 (m), 7.18 (1H, m), 7.10 (m), 2.85 (2H, m), 1.56 (2H, m), 1.23 (18H, m), 0.86 (3H, m).

General Procedure for the Synthesis of Poly[4,4′-bis(alkylthio)-2,2′-bithiophene-5,5′-diyl-*alt*-1,4-phenylene] (P2). They were produced in the same way as **P2′** using $FeCl_3$ as previously reported.[18]

Poly[4,4′-bis(butylthio)-2,2′-bithiophene-5,5′-diyl-*alt*-1,4-phenylene] (P2a): Yield: 83%. ^{1}H NMR: δ 7.74 (4H, m), 7.30 (d), 7.19 (2H, m), 7.10 (d), 2.86 (4H, m), 1.56 (4H, m), 1.38 (4H, m), 0.88 (6H, m). Anal. Calcd for $C_{11}H_{12}S_2$: C, 63.46; H, 5.77; S, 30.77%. Found: C, 62.65; H, 5.65; S, 33.05; Fe, 0.16; Cl, 0.75%.

Poly[4,4′-bis(octylthio)-2,2′-bithiophene-5,5′-diyl-*alt*-1,4-

phenylene] (P2b): Yield: 77%. ^{1}H NMR: δ 7.74 (4H, m), 7.30 (d, $J = 5.1$ Hz), 7.18 (2H, m), 7.10 (d, $J = 5.2$ Hz), 2.85 (4H, m), 1.56 (4H, m), 1.23 (20H, m), 0.86 (6H, m). Anal. Calcd for $C_{15}H_{20}S_2$: C, 68.18; H, 7.58; S, 24.24%. Found: C, 64.85; H, 9.02; S, 27.09; Fe, 0.23; Cl, 1.19%.

Poly[4,4′-bis(dodecylthio)-2,2′-bithiophene-5,5′-diyl-*alt*-1,4-phenylene] (P2c): This polymer was synthesized oxidatively as **P2c′**, starting from **4c**, but only a rubbery material was obtained, even after 40 h. The rubbery crude product was dedoped, dried and then oxidized a second time to offer a dark-green powdery polymer. Yield: 56%. ^{1}H NMR: δ 7.74 (m), 7.19 (m), 7.09 (m), 2.84 (m), 1.55 (m), 1.25 (m), 0.86 (m). Anal. Calcd for $C_{19}H_{28}S_2$: C, 71.25; H, 8.75; S, 20.00%. Found: C, 64.27; H, 7.69; S, 23.44; Fe, 0.13; Cl, 2.21%.

Doping of the Polymer. Polymers were doped by $FeCl_3$ or I_2 as reported earlier.[18,20]

Financial support from National University of Singapore (NUS) under the research grant RP960613 is gratefully acknowledged. JMX is grateful to the NUS for the award of a research scholarship.

References

1 J. R. Elsenbaumer, K. Y. Jen, and R. Oobodi, *Synth. Met.*, **15**, 169 (1986).

2 M. Sato, S. Tanaka, and K. Kaeriyama, *J. Chem. Soc., Chem. Commun.*, **1986**, 873.

3 S.-A. Chen and C.-C. Tsai, *Macromolecules*, **26**, 2234 (1993).

4 M. L. Bolhm, J. E. Pickett, and P. C. V. Dort, *Macromolecules*, **26**, 2704 (1993).

5 X. Wu, T.-A. Chen, and R. D. Rieke, *Macromolecules*, **29**, 7671 (1996).

6 F. Goldoni, D. Iarossi, A. Mucci, L. Schenetti, and M. Zambianch, *J. Mater. Chem.*, **7**, 593 (1997).

7 A. O. Patil, Y. Ikenoue, F. Wudl, and A. J. Heeger, *J. Am. Chem. Soc.*, **109**, 1858 (1987).

8 D. J. Guerrero, X. Ren, and J. P. Ferraris, *Chem. Mater.*, **6**, 1437 (1994).

9 S. Tanaka, M. Sato, and K. Kaeriyama, *Synth. Met.*, **25**, 277 (1988).

10 J. P. Ruiz, K. Nayak, D. S. Marynick, and J. R. Reynolds, *Macromolecules*, **22**, 1231 (1989).

11 C. G. Wang, J. L. Schindler, C. R. Kannewurf, and M. G. Kanatzidis, *Chem. Mater.*, **7**, 58 (1995).

12 J.-L. Bredas in "Handbook of Conducting Polymers," 2nd ed., ed by T. A. Skotheim, Marcel Dekker Inc., New York (1986).

13 R. H. Friend and N. C. Greenham in "Handbook of Conducting Polymers," 2nd ed., ed by T. A. Skotheim, R. L. Elsenbaumer, and J. R. Reynolds, Marcel Dekker Inc., New York, Basel, and Hong Kong (1998).

14 T. J. Kang, J. Y. Kim, K. J. Kim, C. Lee, and S. B. Rhee, *Synth. Met.*, **69**, 377 (1995).

15 A. P. Davey, S. Elliott, O. O'Connor, and W. Blau, *J. Chem. Soc., Chem. Commun.*, **1995**, 1433.

16 J. Li and Y. Pang, *Macromolecules*, **30**, 7487 (1997).

17 S. C. Ng, T. T. Ong, and H. S. O. Chan, *J. Mater. Chem.*, **8**, 2663 (1998).

18 S. C. Ng, J. M. Xu, and H. S. O. Chan, *Synth. Met.*, **92**, 33 (1998).

19 S. C. Ng, J. M. Xu, H. S. O. Chan, A. Fujii, and K. Yoshino, *J. Mater. Chem.*, **9**, 381 (1999).

20 S. C. Ng, J. M. Xu, and H. S. O. Chan, *Macromolecules*, **33**, 7349 (2000).

21 A. Furlani, M. V. Russo, G. Polzonetti, K. Martin, H. H. Wang, and J. R. Ferraro, *Appl. Spectrosc.*, **44**, 331 (1990).

22 M. V. Russo, G. Polzonetti, and A. Furlani, *Synth. Met.*, **39**, 291 (1991).

23 A. Pron, Z. Kucharski, C. Budrowski, M. Zagorska, S. Krichene, J. Suwaiski, G. Dehe, and S. Lefrant, *J. Chem. Phys.*, **83**, 5923 (1985).

24 T. J. Kang, J. Y. Kim, K. J. Kim, C. Lee, and S. B. Rhee, *Synth. Met.*, **69**, 377 (1995).

25 M. Ueda, T. Hayakawa, O. Haba, H. Kawaguchi, and J. Inoue, *Macromolecules*, **30**, 7069 (1997).

26 D. R. Lide, "CRC Handbook of Chemistry and Physics," CRC Press, Boca Raton, Boston, London, New York and Washington D. C. (1998).

27 E. Block, "Reactions of Organosulfur Compounds," Academic Press, New York, San Francisco and London (1982).

28 M. Mastragostino and L. Soddu, *Electrochem. Acta*, **35**, 463 (1990).

29 J. F. Moulder, W. F. Stickle, P. E. Sobol, and K. D. Bomben, "Handbook of X-ray Photoelectron Spectroscopy," Perkin-Elmer, Eden Prairie (1992).

30 E. T. Kang, K. G. Neoh, and K. L. Tan, *Phys. Rew. B*, **44**, 10461 (1991).

31 K. Faid, M. Leclerc, M. Nguyen, and A. Diaz, *Macromolecules*, **28**, 284 (1995).

32 M. C. Gallazzi, L. Castellani, R. A. Marin, and G. Zerbi, *J. Polym. Sci., Part A: Polym. Chem.*, **31**, 3339 (1993).